Journal of Maps

ISSN: (Print) (Online) Journal homepage: https://www.tandfonline.com/loi/tjom20

Geology of the southern Gran Paradiso Massif and Lower Piedmont Zone contact area (middle Ala Valley, Western Alps, Italy)

F. Caso, S. Nerone, A. Petroccia & M. Bonasera

To cite this article: F. Caso, S. Nerone, A. Petroccia & M. Bonasera (2021) Geology of the southern Gran Paradiso Massif and Lower Piedmont Zone contact area (middle Ala Valley, Western Alps, Italy), Journal of Maps, 17:2, 237-246, DOI: 10.1080/17445647.2021.1911869

To link to this article: https://doi.org/10.1080/17445647.2021.1911869

JOURNAL OF MAPS
2021, VOL. 17, NO. 2, 237–246
https://doi.org/10.1080/17445647.2021.1911869

SCIENCE

OPEN ACCESS Check for updates

Geology of the southern Gran Paradiso Massif and Lower Piedmont Zone contact area (middle Ala Valley, Western Alps, Italy)

F. Caso, S. Nerone, A. Petroccia and M. Bonasera

Department of Earth Sciences, University of Turin, Turin, Italy

ABSTRACT

This work presents the structural evolution of a poorly studied key-area in the middle Ala Valley, Western Alps, where two tectono-metamorphic units are exposed. A geological map at the 1:10.000 scale, integrated with meso- and microstructural analysis, has been realised. We investigated the contact area between Gran Paradiso Massif in the footwall and Lower Piedmont Zone in the hanging wall. Both tectono-metamorphic units, with a different paleogeographic affinity, preserve similar polyphasic deformation histories, defined by four deformation phases. The Dp phase, strongly transposing previous structural relicts, is marked by a high-pressure assemblage associated with the Sp foliation. Dp controls the lithological boundary attitude. A mylonitic zone, developed during the Dp, showing kinematic indicators pointing to a top-to-the N-NW sense of shear, is responsible for the juxtaposition of the two units. Dp structural elements are deformed by Dp+1 and Dp+2 subsequent phases. A greenschist-facies overprinting was observed during the Dp+1 phase.

ARTICLE HISTORY
Received 16 December 2020
Revised 23 March 2021
Accepted 24 March 2021

KEYWORDS
Geological mapping; structural geology; polyphase deformation; Western Alps; Gran Paradiso Massif

1. Introduction

The integration of geological mapping, with meso- and microstructural observations, is a fundamental tool needed to reconstruct the geo-structural evolution of orogenic belts (e.g. Gasco et al., 2009; Ghignone, Balestro et al., 2020; Ortolano et al., 2015; Papeschi et al., 2020; Petroccia et al., 2020). The Alpine belt exhibits complex structural patterns to be figured out. In particular, in the Western Alps ophiolitic rocks of the Lower Piedmont Zone (LPZ; Dal Piaz, 1999, 2003 and references therein), directly juxtaposed to the continental basement (the three Internal Crystalline Massifs; Gran Paradiso, Dora Maira and Monte Rosa Massifs), are well exposed. Whereas the Dora Maira and the Monte Rosa Massifs are usually deeply investigated (Compagnoni et al., 2012; Gasco, Borghi, et al., 2011; Gasco, Gattiglio, et al., 2011, 2013; Ghignone, Gattiglio et al., 2020 and references therein), not all sectors of the Gran Paradiso Massif are thoroughly explored under the cartographic point of view (e.g. Beltrando et al., 2008; Gasco & Gattiglio, 2011; Kassem & Ring, 2004; Rosenbaum et al., 2012). Furthermore, very little information is available concerning the structural evolution of tectonic contacts between the ophiolitic rocks and the Internal Crystalline Massifs (Ballèvre & Merle, 1993; Gasco & Gattiglio, 2011; Ghignone, Balestro et al., 2020). This study provides an example of a polyphase tectonic history, occurred during Alpine deformation, and focuses on an unmapped sector of the southern portion of the Gran Paradiso Massif, in the left slope of the middle Ala Valley near Mondrone village, where the tectonic contact between oceanic and continental units crops out.

2. Geological setting

The Alpine chain shows a structural setting marked by a double vergence: European (towards north) in the external sector and Apulian (towards south) in the inner sector. The Western Alps consist of three main structural domains (Dal Piaz, 2001) (Figure 1(a)): (i) the internal domain, corresponding to the Southern Alps; (ii) the external domain, representing the European foreland (Helvetic-Dauphinois domain); (iii) the axial sector of the chain, between the Penninic Front to the north and the Insubric Line to the south. The axial portion represents a composite nappe pile consisting of the Austroalpine and Penninic domains separated by oceanic affinity units of the interposed Piedmont–Ligurian Ocean (Piedmont Zone; Dal Piaz, 1999, 2001; Dal Piaz et al., 2003). The Gran Paradiso Massif (GPM) belongs to the Upper Penninic Domain and together with Monte Rosa and Dora Maira nappes defines the Internal Crystalline Massifs (Schmid et al., 2004) (Figure 1(a)). These elements of the Western Alps crop out as large tectonic windows, overthrust by eclogite-facies meta-ophiolitic units of the Lower Piedmont Zone (LPZ; Dal Piaz,

CONTACT F. Caso fabiola.caso@edu.unito.it Department of Earth Sciences, University of Turin, Via Valperga Caluso 35, Turin 10125, Italy
Supplemental data for this article can be accessed https://doi.org/10.1080/17445647.2021.1911869.

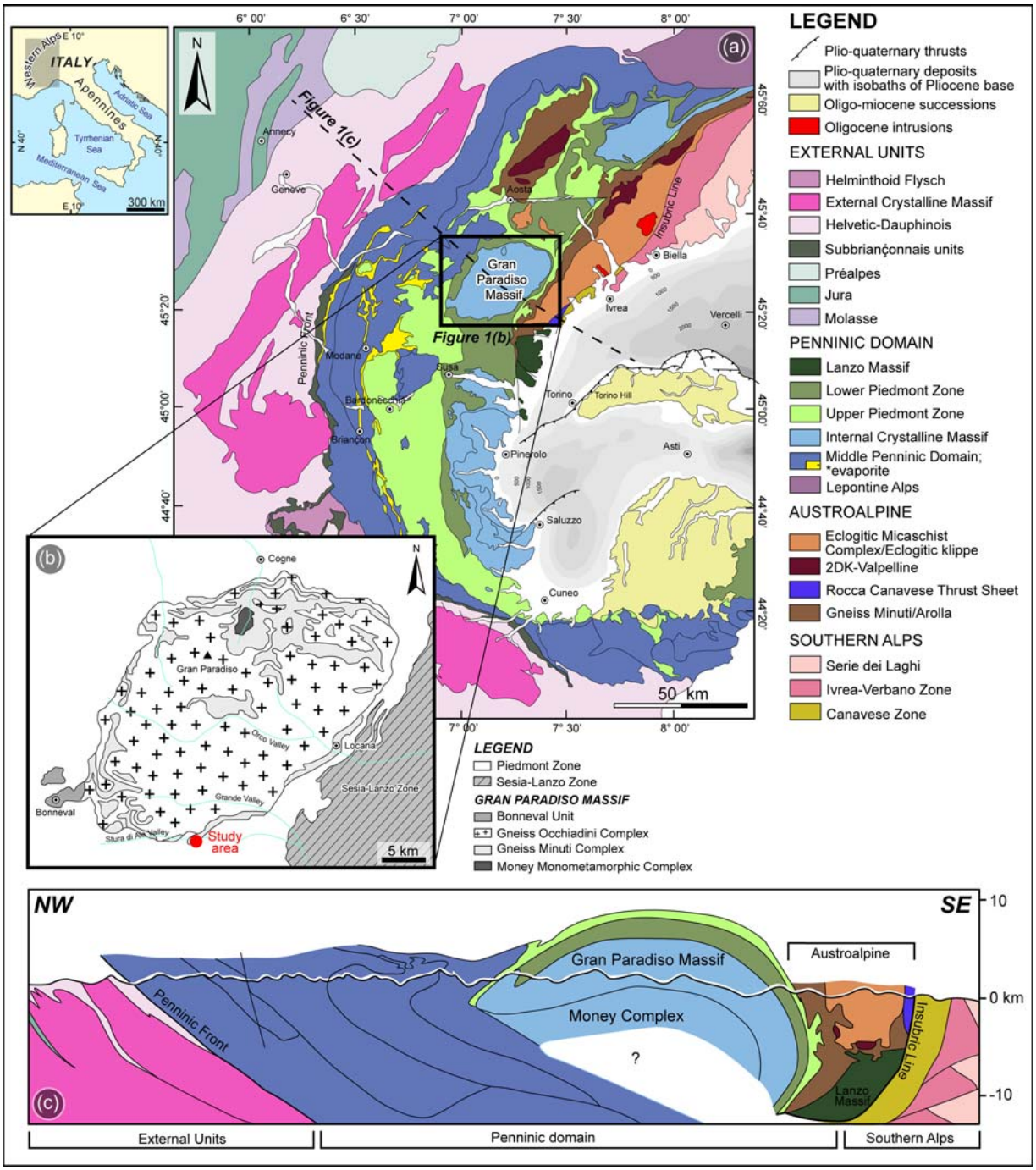

Figure 1. (a) Sketch map of the Western Alps (modified after Piana et al. (2017) and Petroccia et al. (2020)), with its geographic location. (b) Simplified geological map of the Gran Paradiso Massif and neighbouring units (modified after Compagnoni and Lombardo (1974) and Gasco and Gattiglio (2011)). The location of the study area is indicated with a red dot. (c) Simplified cross-section along the Western Alps, across the Gran Paradiso Massif, showing the different tectonic units (modified after Beltrando et al., 2010).

1999; Dal Piaz et al., 2003; Frey et al., 1974) (Figure 1 (b) and (c)). The GPM consists of two main units differing for peak-metamorphism conditions (i.e. eclogitic versus blueschists). The eclogite-facies unit is divided into the Gneiss Minuti (Auct.) Complex and the Gneiss Occhiadini (Auct.) Complex (Compagnoni & Lombardo, 1974; Le Bayon & Ballèvre, 2006). The Gneiss Minuti Complex is made of polymetamorphic paragneiss, micaschist and minor mafic rocks, derived from pre-Alpine amphibolite (Compagnoni & Lombardo, 1974) or late Palaeozoic gabbro (Gasco et al., 2010). The Alpine peak eclogite-facies event (Benciolini et al., 1984; Brouwer et al., 2002) is followed by amphibolite/greenschist-facies condition re-equilibration during decompression (Brouwer et al., 2002; Le Bayon & Ballèvre, 2006). The polymetamorphic basement (Gneiss Minuti Complex) is intruded by porphyritic granitoids of Permian age (270 ± 5 Ma; Bertrand et al., 2005; Ring et al., 2005) metamorphosed into orthogneiss (Gneiss

Occhiadini Complex) during the Alpine orogenesis. The blueschist-facies unit is represented by the Money Monometamorphic Complex (Compagnoni et al., 1974), cropping out as a tectonic window in the northern part of the massif, consisting of metavolcanic and terrigenous rocks (late Carboniferous to early Permian; Manzotti et al., 2015). The metasedimentary cover of the entire massif is represented by Permian metavolcanic rocks (Bonneval Unit; Bertrand, 1968) and by discontinuous lenses of quartzite and marble of Mesozoic age (Elter, 1972).

Based on different metamorphic evolution and lithostratigraphic setting, meta-ophiolitic units of the Western Alps have been classically distinguished into the blueschists-facies Upper Piedmont Zone (UPZ; Agard et al., 2001) and the eclogite-facies Lower Piedmont Zone (e.g. the Orsiera Rocciavrè ophiolites: Pognante, 1979; the Monviso meta-ophiolite complex: Lardeaux et al., 1987). These units are separated by a regional-scale shear zone (e.g. Susa Shear Zone; Ghignone, Gattiglio et al., 2020, 2020; Combin Fault; Ballèvre & Merle, 1993). The UPZ is represented by calcschists with intercalations of metabasalt and serpentinite. The LPZ is mainly made by oceanic crust, represented by serpentinite with minor peridotite, including discontinuous bodies of Mg–Al to Fe–Ti-rich metagabbro and overlaid by metabasalt (Ghignone, Balestro et al., 2020; Groppo & Castelli, 2010; Locatelli et al., 2019). Locally a thin metasedimentary cover composed of impure quartzite, micaschist, marble and calcschist is preserved.

3. Methods

A geological survey of an area of about 14 km^2 has been performed at 1:5.000 scale. New 10 m contour lines have been obtained using the LiDAR-derived DTM with 5 m grid resolution (DTM LiDAR 2009–2011 Piemonte ICE), integrated into a WGS 84, UTM 32N GIS spatial database to derive a Hillshade map. The geological map (see Main Map) has been realised at 1:10.000 scale. Structures were classified according to Passchier and Trouw (2005). A not-numerical progression has been used for the description of deformation phases and the associated structural elements to avoid confusion with the literature and existing knowledge. Abbreviation S for syn-metamorphic surfaces or axial plane foliation of folds, A for fold axes, L for object lineations, F for folds and D for the deformative events have been used. The suffix 'p' denotes 'principal'. All the collected structural elements have been plotted in equal-area stereo diagrams in the lower hemisphere. Mineral abbreviations are after Whitney and Evans (2010). Microstructural analysis on oriented thin sections, cut parallel to the object lineation and perpendicular to the main foliation (XZ plane of the strain ellipsoid) has been performed. The cross-sections (A-A' and B-B'; see Main Map) have been drawn perpendicular to the main structures.

4. Lithostratigraphy

The investigated area is located on the left orographic side of Ala Valley, an E-W trending valley, forming part of Stura di Ala Stream more articulated drainage basin. Its course does not have any relevant, persistent tributary in the investigated segment. The altitude range is between about 2700 m a.s.l., which is the average height of the reliefs located at the western watershed with Grande Valley, and about 1200 m a.s.l. in the valley floor nearby Mondrone village. In the north-western sector of the study area augen-orthogneiss (Go; Gneiss Occhiadini Complex) and paragneiss (Gm; Gneiss Minuti Complex), belonging to the GPM, crop out. The augen-orthogneiss outcrops as discontinuous, decametric lenses in the paragneiss of the Gneiss Minuti Complex. They are coarse-grained rocks characterised by a spaced disjunctive mm-thick foliation defined by the alternation of white mica-rich and quartz- plus feldspar-rich levels. Micaceous levels wrap around pluri-millimetric to pluri-centimetric K-feldspar asymmetric σ- or δ-porphyroclasts (Figure 2(a)). Locally thin and unmappable layers of micaschist are present. Paragneiss belonging to the Gneiss Minuti Complex shows a less-spaced foliation made by micaceous levels alternating with mm-thick quartz- plus feldspar-rich ones (Figure 2(b)). Locally, both symmetric and asymmetric, pluri-millimetric quartz or felspar porphyroclasts, wrapped by the main foliation, are present. Generally, GPM rocks are characterised by a later static growth of chlorite and epidote on previous minerals. Centimetre- to metre-thick and unmappable layers of micaschist, which grade to paragneiss are locally present.

The LPZ in the study area is represented by serpentinite, metagabbro and metabasite. Serpentinite (Sr) is well-foliated but locally presents a massive structure. The main foliation is defined by alternating millimetric serpentine-rich and dark magnetite-rich layers. Metagabbro (Mg) crops out in decametric lenses embedded in serpentinite and metabasite. It is mainly composed of pluri-millimetric greenish clinopyroxene, locally replaced by amphibole, wrapped by a continuous foliation made of fine-grained epidote, pyroxene and minor amphibole (Figure 2(c)). Metabasite (Mb) has a banded structure made of alternating levels of pluri-millimetric garnet porphyroblasts, omphacite-rich and blue amphibole-rich levels (Figure 2(d)). Locally, blue amphibole is replaced by green amphibole around the rim.

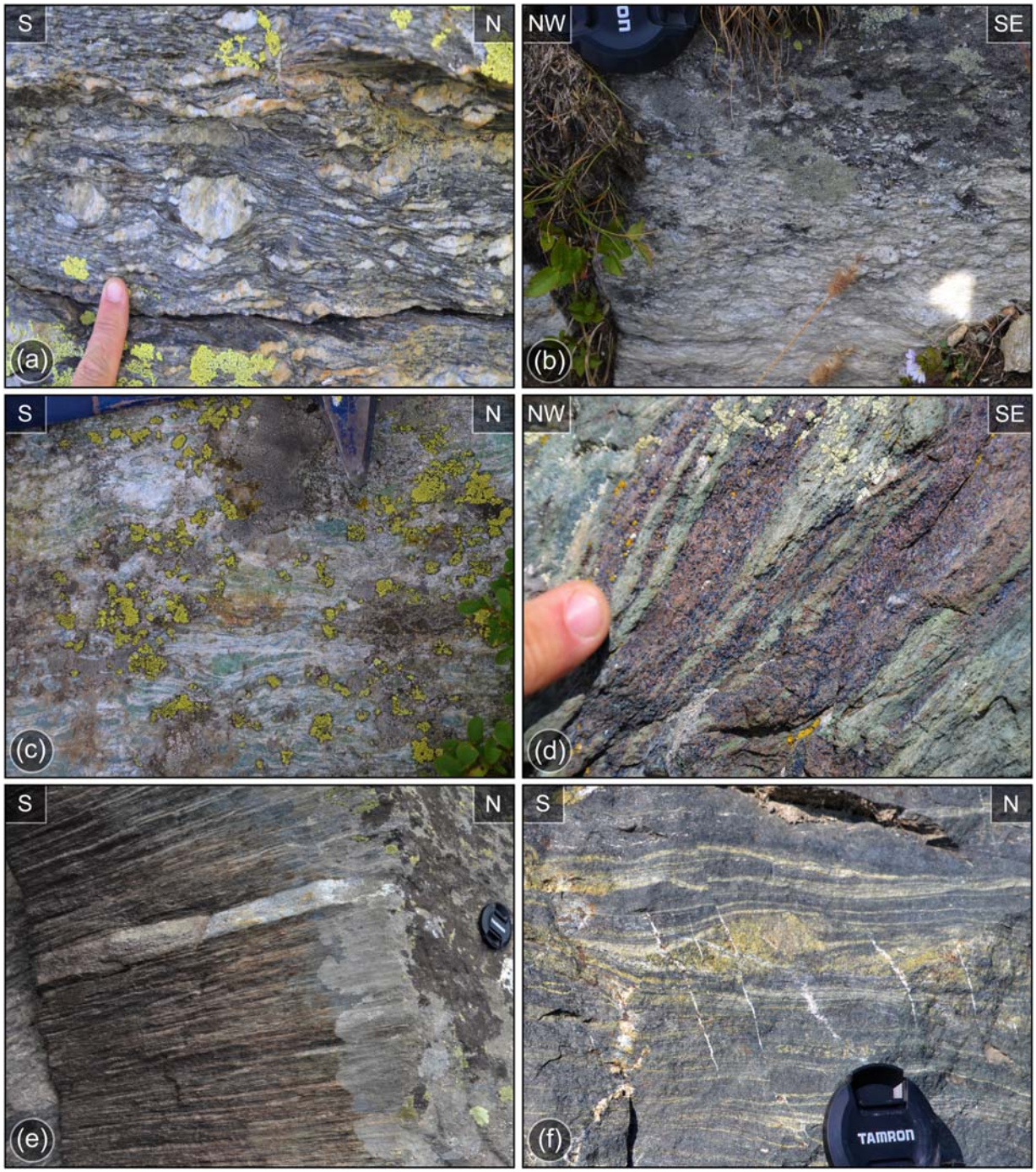

Figure 2. (a) Coarse-grained augen-orthogneiss belonging to the Gneiss Occhiadini Complex. (b) Fine-grained paragneiss of the Gneiss Minuti Complex. (c) Outcrop evidence of mylonitic metagabbro of the Lower Piedmont Zone. (d) Metabasite characterised by alternating reddish garnet, greenish clinopyroxene-rich and blue amphibole-rich levels. (e) Gran Paradiso Massif flaser-gneiss near the tectonic contact. (f) Top-to-the N sense of shear evidence in metabasite.

The tectonic contact between the GPM and the LPZ is highlighted by a centimetre- to metre-thick mylonitic zone, which cannot be represented in our map due to its scale. Non-coaxial deformation affected rocks belonging to both units, with a major extension in the GPM, whose lithologies are locally heterogeneously deformed, displaying flaser-gneiss structure (Figure 2(e)). Mylonites show a grain-size reduction and an increase of kinematic indicators moving toward the high-strain zone (Figure 2(f)).

5. Structural evolution

Geological mapping, meso- and microstructural analyses pointed out that the LPZ and GPM are affected by a similar polyphase deformation history which can be divided into four phases. A synoptic summary table of the deformational structures events accompanied by mineral assemblages for each lithotype is reported in Table 1.

The first tectonic phase (Dp-1), due to the strongly superposed Dp structures in most of the area, is

Table 1. Summary table displaying the deformational structures and the mineral assemblages for each lithology.

	Protolith-relict	Dp-1	Dp	Dp+1	Dp+2
METABASITE	-	No preserved plicative structures Sp-1 = Gln +Wm+Omp+Grt+Rt	Transpositive phase with rootless and isoclinal folds Top-to-the NW sense of shear Sp = Gln+Rt+Grt+Opq	Gentle asymmetric folds Δ = Brownish- and green-Amp+Ep +Ttn No detected Sp+1 foliation	Open folds No blastesis
METAGABBRO	Magmatic Px	No preserved plicative structures Coronitic Omp	Transpositive phase Top-to-the NW sense of shear Sp = Omp+Zo+Gln	Close folds Sp+1 = Chl+Ep +Green Amp	No blastesis
SERPENTINITE	-	-	Transpositive phase Sp = Srp+Tr +Mag	Kink, chevron, closed to tight folds Sp+1 = Srp+Chl+Tr	Open folds No blastesis
AUGEN-ORTHOGNEISS	Magmatic Kfs +Pl+Bt+Qz	No preserved plicative structures	Transpositive phase with rootless and isoclinal folds Top-to-the N-NW sense of shear Sp = Wm+Qz+Ep +Opq	Gentle asymmetric folds Δ = Ep +Wm+Bt No detected Sp+1 foliation	No blastesis
PARAGNEISS	-	No preserved plicative structures	Transpositive phase with rootless folds Top-to-the N-NW sense of shear Sp = Wm+Qz+Zo+Opq	Kink, chevron and asymmetric folds Δ = Ep+Chl+Wm+Ab No detected Sp+1 foliation	Open and box folds No blastesis

associated with the development of a relict foliation preserved only in the hinges of mesoscopic rootless and isoclinal folds in more competent layers (Sp-1; Figure 3(a) and (b)), which are not entirely transposed. Dp-1 microscale evidence has been detected only in metabasite, defined by the random occurrence of Gln + Wm + Omp + Grt + Rt (Figure 3(c)), and in metagabbro marked by omphacite rims around the magmatic pyroxene.

Dp folds (Fp) vary from pluri-centimetric to pluri-kilometric and their geometry is strictly controlled by the rheology of each involved lithology, varying from tight, isoclinal to rootless, with rounded and thickened hinges and stretched limbs (class 2 of Ramsay (1967); B5 according to Hudleston (1973)). They occur mainly as a medium- and small-scale structures, but also at the cartographic scale (see Main Map). Ap axes and intersection lineations between Sp foliation and folded Sp-1 surfaces show a main NE-SW strike, moderately dipping toward NE and SW. The Dp phase gave rise to the most prominent structures of the investigated area. Parallel to Fp axial planes, an Sp axial plane foliation driving the lithological contacts attitude has been recognised. Sp is continuous and well developed in weak lithologies, while it is observable as a spaced disjunctive cleavage in more competent ones. In thin section, the Sp both in LPZ and GPM is mainly marked by high-pressure assemblages (Table 1). A prime example is present in metagabbro where the Sp is defined by Omp + Zo + Gln wrapping around magmatic pyroxene (Figure 3(d)). This main planar element (Sp) shows a general NE-SW strike and mainly dips toward SE in the south-eastern and north-western part, and toward NW in the central part of the investigated area. Dip angles range between 10° and 70°, with higher values observed in the central part whereas lower values occur at the marginal portions of the map (Figure 3(a) and (b)). The Lp object lineation is represented by both grain and aggregate lineation. Lp becomes prominent as the shearing deformation increases. Lp trends about NW-SE and plunges towards SE and NW, nearly perpendicular to Ap fold axes. The lithologies located far from the tectonic contact area show few if any, kinematic indicators, whereas, approaching the tectonic contact, they become more frequent and Sp shows a transition from a Dp axial plane foliation to a mylonitic foliation. Shear sense indicators have been observed at the mesoscale on section approximating the XZ plane of the finite strain ellipsoid (i.e. perpendicular to the Sp foliation and parallel to the Lp lineation). The main kinematic indicators are represented by C–S and C'–S fabrics (Figure 3(e)), σ- and δ-type porphyroclasts and mica-fish (Figure 3(f)). All the kinematic indicators indicate a top-to-the N-NW normal sense of shear.

The subsequent Dp+1 deformation event is strongly controlled by the rheology of each lithology, indeed it is mainly evident in foliated serpentinites (Figure 4(a)). The Fp+1 folds range from centimetric to metric in scale. The inter-limb angle of the folds varies considerably; the folds may be close to tight, mainly in serpentinites or open to gentle in other lithologies. Rare kink, chevron and/or asymmetric Fp+1 folds occur also in the Gran Paradiso Massif units. Ap+1 fold axes are generally coaxial to Ap ones but showing higher plunging values (Figure 4 (a)). An Sp+1 axial plane foliation, striking from NE-SW to E-W, is rarely observable at the meso- and microscale. A spaced crenulation cleavage has been recognised in serpentinite and metagabbro only. In all the lithologies, during this stage, an intense metamorphic overprinting by greenschist-facies minerals on previous high-pressure assemblage has been observed (Table 1) (Figure 4(b)).

Neither axial plane foliation nor blastesis has been recognised during the Dp+2 deformation phase. The Fp+2 corresponds to open or box folds, ranging from metric to decametric in size, with sub-horizontal to gently dipping axes and axial planes. Ap+2 axes plunge at low angles toward ENE or WSW with very high-scattered values (Figure 4(c) and (d)). Both Fp

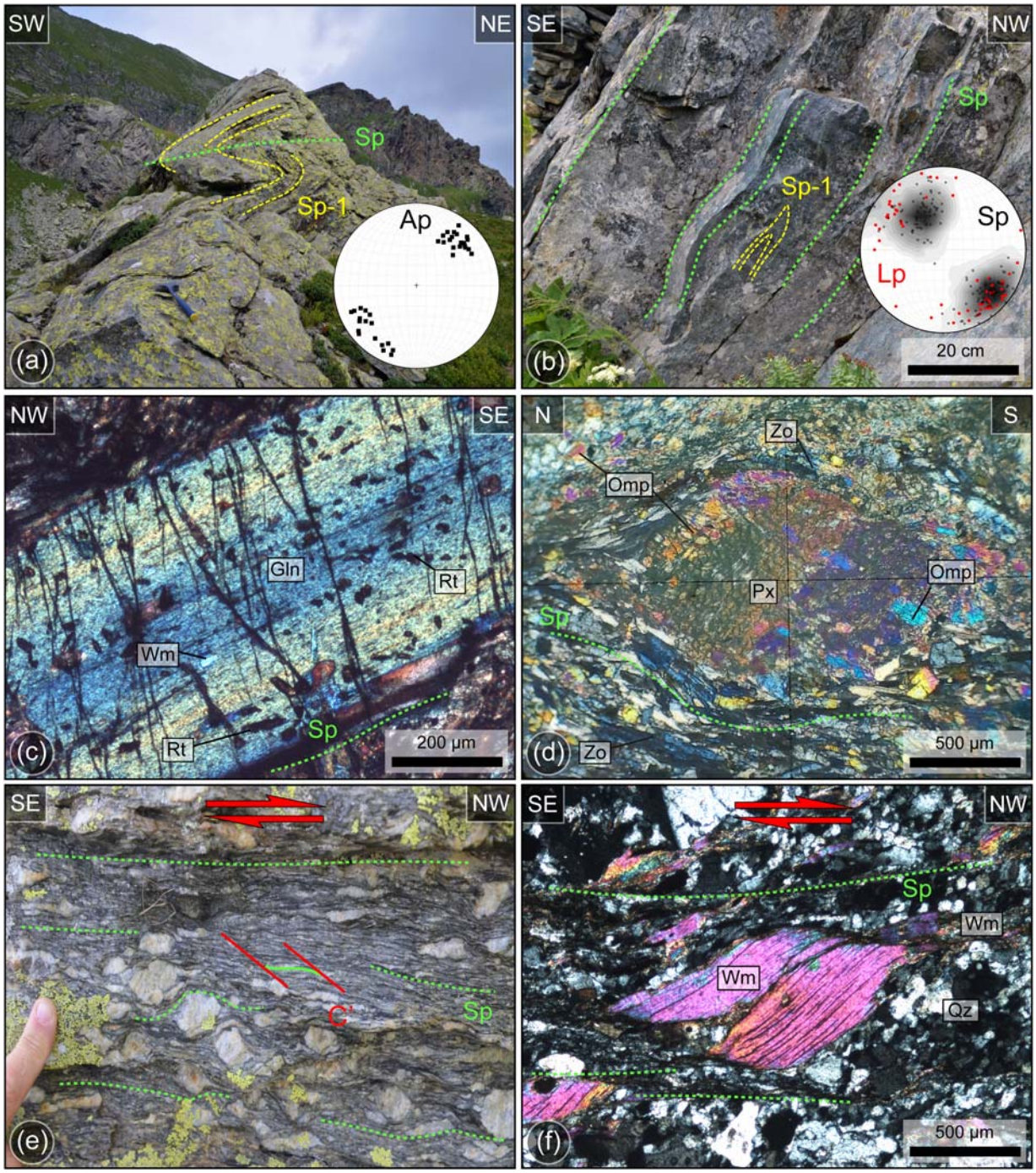

Figure 3. Ductile structures with stereographs of the main elements. (a) Isoclinal Dp fold developed in augen-orthogneiss deforming an older Sp-1 foliation. (b) Dp fold affecting metabasite and deforming a relict Sp-1 foliation. (c) Glaucophane along the Sp foliation including an Sp-1 defined by Rt + Wm (XPL: cross-polarized light). (d) Magmatic pyroxene with a corona of omphacite, wrapped by the Sp foliation, defined by Omp + Zo (XPL). (e) C′-S fabric with a top-to-the NW sense of shear and σ-porphyroclast in augen-orthogneiss. (f) Microphotograph of a mica-fish in augen-orthogneiss indicating a top-to-the NW sense of shear (XPL).

+1 and Fp+2 folds show coaxiality with the Dp structures. The Dp+2 deformation phase is responsible for the re-orientation of the original attitude of the previous structural elements.

6. Geomorphological features and quaternary evolution

Traces of the Pleistocene glacial modelling, linked to the last phase of maximum expansion, are testified by lateral morainic deposits of the main glacier and by small glacial cirques upstream, probably sources of short, tributary glaciers. The slope is gentle in its lowest part (the left side of a U-shaped valley) and characterised by two slow, large, complex landslides involving till deposits (g2), occasionally uncovered. The two mapped movements act as conveyor belts for large dimension, serpentinite-metabasite boulders, heavily weathered by glacial erosion and progressively carried downstream.

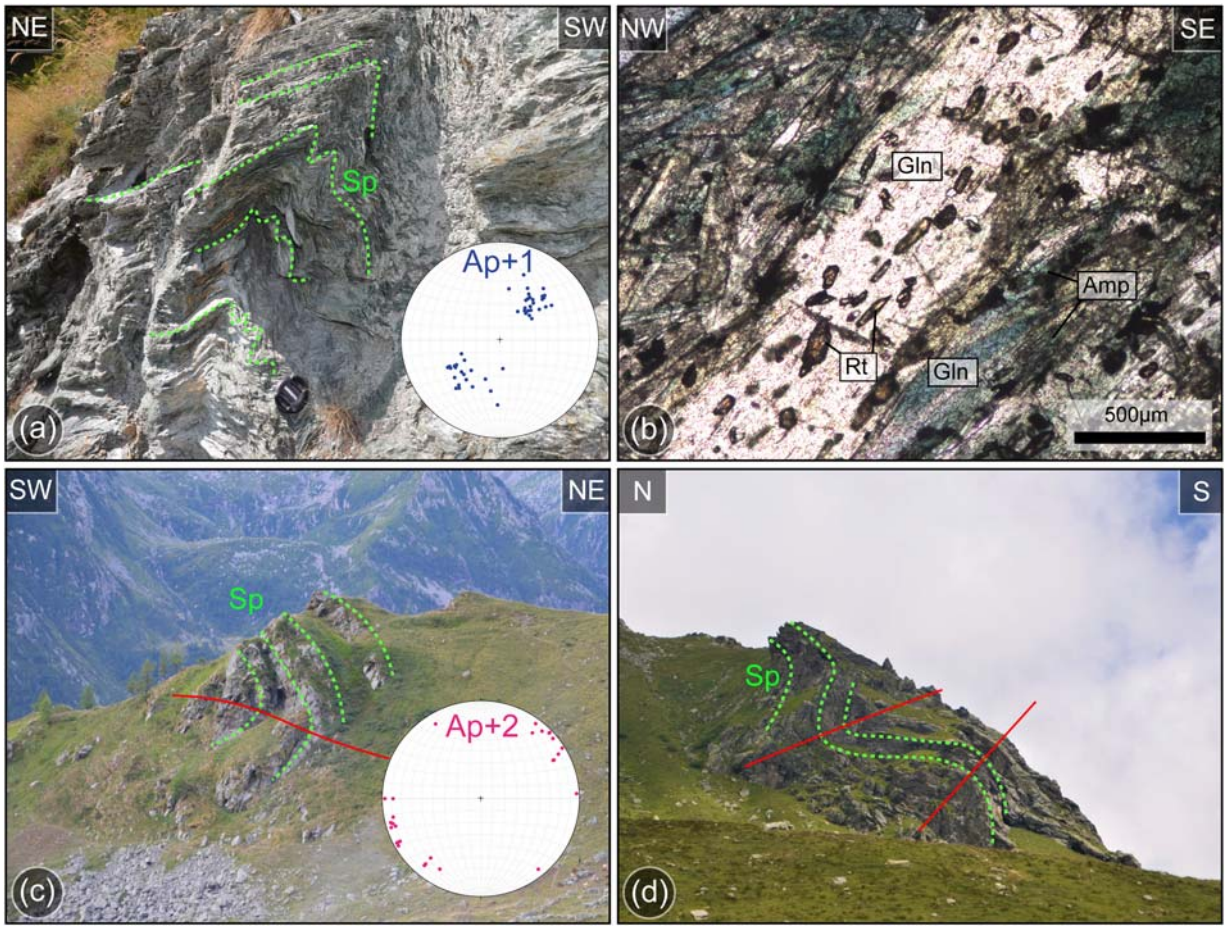

Figure 4. Post-Sp ductile structures with stereographs of the main elements. (a) Dp+1 folds developed in serpentinite. (b) Blastesis of green amphibole on syn-Dp glaucophane in metabasite (PPL: plane-polarized light). (c,d) Late open folds (Dp+2) with sub-horizontal axes and axial planes deforming the main foliation (Sp).

Remnants of the above-mentioned, gentle landscape are incised by the recent hydrographic pattern developed in response to the new Holocene base level of the Stura di Ala Stream (Figure 5(a)). The relief energy increases in the highest part of the slope, where a great quantity of debris (g1) develops in the proximity of the very fractured ridges, producing material for debris and rock flows (Figure 5(b)). Their emplacement is coupled with Stura di Ala alluvial deposits (m) of the valley floor, on which Mondrone and Martassina villages are founded. Despite slope and glacial deposits are spread over the mapped area, in the Main Map we chose to draw just quaternary deposits with an observable thickness larger than 3 metres. For this reason, the bedrock has not been covered by morainic deposits at all and debris flows and avalanches thickest accumulation bodies have been merged with alluvial sediments.

7. Final remarks

The new geological map (see Main Map) at 1:10.000 scale is the most detailed, currently available representation of the geological and structural setting of the Mondrone area (middle Ala Valley, Piedmont). Two juxtaposed tectono-metamorphic units have been distinguished (Figure 6(a)): the lower one represented by the Gran Paradiso Massif and the upper one testified by the oceanic Lower Piedmont Zone. In both units, a complex polyphase evolution (Figure 6(b)), defined by four ductile deformation phases, has been detected. The most prominent deformation phase Dp is responsible for the development of the main foliation, pervasive at all scales (Sp) that generally transposed the previous Sp-1. It becomes mylonitic moving toward the boundary between the two units, showing several kinematic indicators with a top-to-the NW normal sense of shear. A syn-kinematic high-pressure mineral assemblage parallel to the Sp mylonitic foliation has been recognised in both units. Pre-Dp mineralogical high-pressure relicts are still present, particularly in LPZ. All the previous structural elements are widely deformed by the two last deformation events (Dp+1 and Dp+2), the latter causing the overturning of the Sp dip direction from SE to NW and a topographic interference (Figure 6(b)). The syn-kinematic greenschist-facies minerals (Dp+1), generally grown at the expense of high-pressure

Figure 5. (a) V-valley incising the older shaped-by-ice, gentle slope. (b) Debris deposits lying around fractured rock walls in the northernmost part of the mapped area.

assemblages, testifies a changing in metamorphism from Dp to Dp+1. The obtained data are consistent with the coupling of LPZ with GPM during HP conditions (Dp-1 and Dp) and a subsequent uplift up to greenschist-facies conditions (Dp+1; Beltrando et al., 2010; Gasco et al., 2010). The last stage of deformation (Dp+2) causes open and box fold with neither axial plane foliation nor blastesis.

The mapping of the Quaternary cover allowed assuming the presence of a widespread scree slope and two large gravitational accumulation bodies.

The new and updated geological information about this inner sector of the Alpine belt begins to fill the gap about mapping and inferring tectono-metamorphic evolution of this area and encourages future detailed investigations.

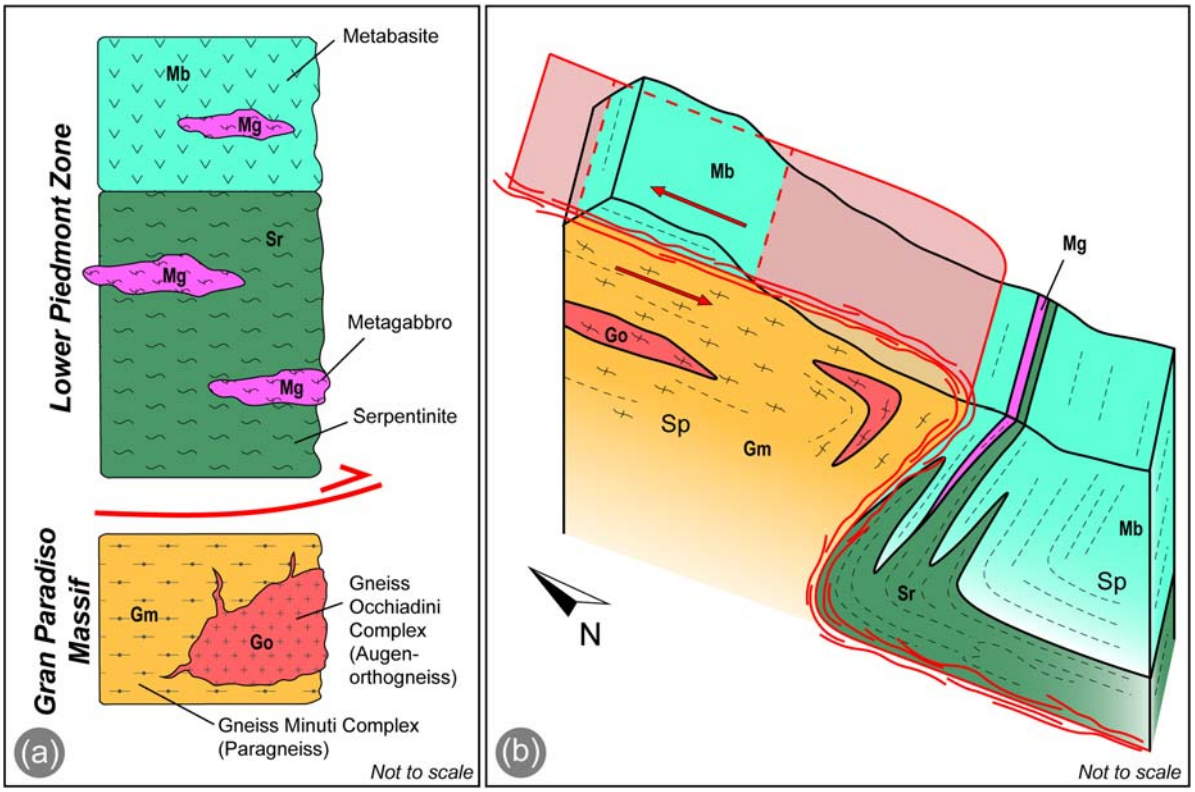

Figure 6. (a) Schematic stratigraphic column of the Gran Paradiso Massif and the overlying Lower Piedmont Zone in the study area. Gm: Gneiss Minuti Complex; Go: Gneiss Occhiadini Complex; Sr: Serpentinite; Mg: Metagabbro; Mb: Metabasite. (b) Schematic geological model of the study area showing the possible structural interpretation. In this sector, the influence of the Dp+2 deformation phase with sub-horizontal axial planes is evident, as it is responsible for the overturning of the Sp foliation and of the tectonic contact. The latter is represented as a mylonitic zone showing kinematic indicators with a top-to-the N-NW sense of shear, affecting both the Gran Paradiso Massif and the Lower Piedmont Zone.

8. Software

The map has been drawn using QGis 3.12 Buçuresti, and its final assemblage has been realised with Adobe Illustrator® CC 2018. Structural data have been plotted with the software Stereonet© 10.

9. Geolocation information

The study area is located in the middle Ala Valley, near Mondrone village, in the Western Alps (Piedmont, northwestern Italy). The area is placed between 5022600–362400 and 5019000 –364800; coordinate system: WGS 1984 / UTM Zone 32 N.

Acknowledgements

Many thanks to Prof. Gaetano Ortolano, Prof. Laura Federico and Prof. Giedre Beconyte for their helpful reviews and Dr. Mike J Smith for his excellent editorial job.

Disclosure statement

No potential conflict of interest was reported by the author(s).

Data availability statement

The authors confirm that the data supporting the findings of this study are freely available within the article and its supplementary materials.

ORCID

F. Caso http://orcid.org/0000-0002-1136-2811
S. Nerone http://orcid.org/0000-0001-7277-2454
A. Petroccia http://orcid.org/0000-0001-5230-0046
M. Bonasera http://orcid.org/0000-0003-1580-2519

References

Agard, P., Jolivet, L., & Goffe, B. (2001). Tectonometamorphic evolution of the Schistes Lustres complex: Implications for the exhumation of HP and UHP rocks in the western Alps. *Bulletin de la Société Géologique de France*, *172*(5), 617–636. https://doi.org/10.2113/172.5.617

Ballèvre, M., & Merle, O. (1993). The combin fault: Reactivation of a late cretaceous-early tertiary detachment fault in the Western Alps. *Schweizerische Mineralogische und Petrologische Mitteilungen*, *73*(2), 205–227.

Beltrando, M., Compagnoni, R., & Lombardo, B. (2010). (Ultra-) High-pressure metamorphism and orogenesis: An Alpine perspective. *Gondwana Research*, *18*(1), 147–166. https://doi.org/10.1016/j.gr.2010.01.009

Beltrando, M., Lister, G., Hermann, J., Forster, M., & Compagnoni, R. (2008). Deformation mode switches in the Penninic units of the Urtier Valley (Western Alps): Evidence for a dynamic orogen. *Journal of Structural Geology*, *30*(2), 194–219. https://doi.org/10.1016/j.jsg.2007.10.008

Benciolini, L., Martin, S., & Tartarotti, P. (1984). Il metamorfismo eclogitico nel basamento del Gran Paradiso ed in unità piemontesi della valle di campiglia. *Memorie Della Società Geologica Italiana*, *29*, 127–151.

Bertrand, J. M. (1968). Etude structurale du versant occidental du Massif du Grand Paradis (Alpes Graïes). *Géologie Alpine*, *44*, 57–87. http://geologie-alpine.ujf-grenoble.fr/articles/GA_1968__44__55_0.pdf

Bertrand, J. M., Paquette, J. L., & Guillot, F. (2005). Permian zircon U–Pb ages in the Gran Paradiso massif: Revisiting post- Variscan events in the Western Alps. *Schweizerische Mineralogische und Petrologische Mitteilungen*, *85*(1), 15–29. https://hal.archives-ouvertes.fr/hal-00177470

Brouwer, F. M., Vissers, R. L. M., & Lamb, W. M. (2002). Structure and metamorphism of the Gran Paradiso massif, Western Alps, Italy. *Contributions to Mineralogy and Petrology*, *143*(4), 450–470. https://doi.org/10.1007/s00410-002-0357-6

Compagnoni, R., Elter, G., & Lombardo, B. (1974). Eterogeneità stratigrafica del complesso degli "Gneiss Minuti" nel massiccio cristallino del Gran paradiso. *Memorie Della Società Geologica Italiana*, *13*, 227–239.

Compagnoni, R., & Lombardo, B. (1974). The Alpine age of the Gran Paradiso eclogites. *Rendiconti Della Società Italiana di Mineralogia e Petrografia*, *30*, 223–237.

Compagnoni, R., Rolfo, F., Groppo, C., Hirajima, T., & Turello, R. (2012). Geologic map of the UHP Brossasco-Isasca Unit (Western Alps). *Journal of Maps*, *8*(4), 465–472. https://doi.org/10.1080/17445647.2012.744367

Dal Piaz, G. V. (1999). The austroalpine-Piedmont nappe stack and the puzzle of Alpine Tethys. *Memorie di Scienze Geologiche*, *51*(1), 155–176.

Dal Piaz, G. V. (2001). History of tectonic interpretations of the Alps. *Journal of Geodynamics*, *32*(1–2), 99–114. https://doi.org/10.1016/S0264-3707(01)00019-9

Dal Piaz, G. V., Bistacchi, A., & Massironi, M. (2003). Geological outline of the Alps. *Episodes*, *26*(3), 175–180. https://doi.org/10.18814/epiiugs/2003/v26i3/004

Elter, G. (1972). Contribution à la connaissance du briançonnais interne et de la bordure piémontaise dans les Alpes Graies nord-orientales et considérations sur les rapports entre les zones du briançonnais et des Schistes lustrés. *Memorie Degli Istituti di Geologia e Mineralogia Dell'Università di Padova*, *28*, 1–18.

Frey, M., Hunziker, J. C., Frank, W., Bocquet, J., Dal Piaz, G. V., Jäger, E., & Niggli, E. (1974). Alpine metamorphism of the Alps. A review. *Schweizerische Mineralogische und Petrologische Mitteilungen*, *54*, 247–290.

Gasco, I., Borghi, A., & Gattiglio, M. (2010). Metamorphic evolution of the Gran Paradiso Massif: A case study of an eclogitic metagabbro and a polymetamorphic glaucophane–garnet micaschist. *Lithos*, *115*(1–4), 101–120. https://doi.org/10.1016/j.lithos.2009.11.009

Gasco, I., Borghi, A., & Gattiglio, M. (2011a). P–T Alpine metamorphic evolution of the Monte Rosa nappe along the Piedmont Zone boundary (Gressoney Valley, NW Italy). *Lithos*, *127*(1–2), 336–353. https://doi.org/10.1016/j.lithos.2011.09.007

Gasco, I., & Gattiglio, M. (2011b). Geological map of the middle Orco Valley, Western Italian Alps. *Journal of Maps*, *7*(1), 463–477. https://doi.org/10.4113/jom.2010.1121

Gasco, I., Gattiglio, M., & Borghi, A. (2009). Structural evolution of different tectonic units across the austroalpine–Penninic boundary in the middle Orco Valley (Western

Italian Alps). *Journal of Structural Geology*, *31*(3), 301–314. https://doi.org/10.1016/j.jsg.2008.11.007

Gasco, I., Gattiglio, M., & Borghi, A. (2011c). Lithostratigraphic setting and P-T metamorphic evolution for the Dora Maira Massif along the Piedmont Zone boundary (middle Susa Valley, NW Alps). *International Journal of Earth Sciences*, *100*(5), 1065–1085. https://doi.org/10.1007/s00531-011-0640-8

Gasco, I., Gattiglio, M., & Borghi, A. (2013). Review of metamorphic and kinematic data from Internal Crystalline Massifs (Western Alps): PTt paths and exhumation history. *Journal of Geodynamics*, *63*, 1–19. https://doi.org/10.1016/j.jog.2012.09.006

Ghignone, S., Balestro, G., Gattiglio, M., & Borghi, A. (2020a). Structural evolution along the Susa Shear Zone: The role of a first-order shear zone in the exhumation of meta-ophiolite units (Western Alps). *Swiss Journal of Geosciences*, *113*(17), 1–16. https://doi.org/10.1186/s00015-020-00370-6

Ghignone, S., Gattiglio, M., Balestro, G., & Borghi, A. (2020b). Geology of the Susa Shear Zone (Susa Valley, Western Alps). *Journal of Maps*, *16*(2), 79–86. https://doi.org/10.1080/17445647.2019.1698473

Groppo, C., & Castelli, D. (2010). Prograde P-T evolution of a lawsonite eclogite from the Monviso meta-ophiolite (Western Alps): dehydration and redox reactions during subduction of oceanic FeTi-oxide gabbro. *Journal of Petrology*, *51*(12), 2489–2514. https://doi.org/10.1093/petrology/egq065

Hudleston, P. (1973). Fold morphology and some geometrical implications of theories of fold development. *Tectonophysics*, *16*(1-2), 1–46. https://doi.org/10.1016/0040-1951(73)90129-7

Kassem, O. K., & Ring, U. (2004). Underplating-related finite-strain patterns in the Gran Paradiso massif, Western Alps, Italy: Heterogeneous ductile strain superimposed on a nappe stack. *Journal of the Geological Society*, *161*(5), 875–884. https://doi.org/10.1144/0016-764903-159

Lardeaux, J. M., Nisio, P., & Boudeulle, M. (1987). Deformational and metamorphic history at the lago superiore area of the Monviso ophiolitic complex (Italian western Alps): a record of subduction-collision cycle? *Ofioliti*, *12*(3), 479–502.

Le Bayon, B., & Ballèvre, M. (2006). Deformation history of a subducted continental crust (Gran Paradiso, Western Alps): continuing crustal shortening during exhumation. *Journal of Structural Geology*, *28*(5), 793–815. https://doi.org/10.1016/j.jsg.2006.02.009

Locatelli, M., Federico, L., Agard, P., & Verlaguet, A. (2019). Geology of the southern Monviso metaophiolite complex (W-Alps, Italy). *Journal of Maps*, *15*(2), 283–297. https://doi.org/10.1080/17445647.2019.1592030

Manzotti, P., Pitra, P., Langlade, J., & Ballèvre, M. (2015). Constraining P–T conditions during thrusting of a higher pressure unit over a lower pressure one (Gran Paradiso, Western Alps). *Journal of Metamorphic Geology*, *33*(9), 981–1002. https://doi.org/10.1111/jmg.12156

Ortolano, G., Cirrincione, R., Pezzino, A., Tripodi, V., & Zappala, L. (2015). Petro-structural geology of the eastern aspromonte Massif crystalline basement (southern Italy-calabria): an example of interoperable geo-data management from thin section – to field scale. *Journal of Maps*, *11*(1), 181–200. https://doi.org/10.1080/17445647.2014.948939

Papeschi, S., Iaccarino, S., & Montomoli, C. (2020). Underthrusting and exhumation of continent-derived units within orogenic wedge: An example from the Northern Apennines (Italy). *Journal of Maps*, *16*(2), 638–650. https://doi.org/10.1080/17445647.2020.1795736

Passchier, C. W., & Trouw, R. A. J. (2005). *Microtectonics*. Springer-Verlag Berlin Heidelber. https://doi.org/10.1007/3-540-29359-0

Petroccia, A., Bonasera, M., Caso, F., Nerone, S., Morelli, M., Bormioli, D., & Moletta, G. (2020). Structural and geomorphological framework of the upper Maira Valley (Western Alps, Italy): the case study of the Gollone Landslide. *Journal of Maps*, *16*(2), 534–542. https://doi.org/10.1080/17445647.2020.1784806

Piana, F., Fioraso, G., Irace, A., Mosca, P., D'Atri, A., Barale, L., Falletti, P., Monegato, G., Morelli, M., Tallone, S., & Vigna, G. B. (2017). Geology of Piemonte region (NW Italy, Alps–Apennines interference zone). *Journal of Maps*, *13*(2), 395–405. https://doi.org/10.1080/17445647.2017.1316218

Pognante, U. (1979). The orsiera-Rocciavrè metaophiolitic complex (Italian Western Alps). *Ofioliti*, *4*, 183–198.

Ramsay, J. G. (1967). *Folding and fracturing of rocks*. Mcgraw-Hill.

Ring, U., Collins, A. S., & Kassem, O. K. (2005). U–Pb SHRIMP data on the crystallization age of the Gran Paradiso augengneiss, Italian Western Alps: Further evidence for Permian magmatic activity in the Alps during break-up of Pangea. *Eclogae Geologicae Helvetiae*, *98*(3), 363–370. https://doi.org/10.1007/s00015-005-1170-9

Rosenbaum, G., Menegon, L., Glodny, J., Vasconcelos, P., Ring, U., Massironi, M., Thiede, D., & Nasipuri, P. (2012). Dating deformation in the Gran Paradiso Massif (NW Italian Alps): implications for the exhumation of high-pressure rocks in a collisional belt. *Lithos*, *144–145*, 130–144. https://doi.org/10.1016/j.lithos.2012.04.016

Schmid, S. M., Fügenschuh, B., Kissling, E., & Schuster, R. (2004). Tectonic map and overall architecture of the Alpine orogen. *Eclogae Geologicae Helvetiae*, *97*(1), 93–117. https://doi.org/10.1007/s00015-004-1113-x

Whitney, D. L., & Evans, B. W. (2010). Abbreviations for names of rock-forming minerals. *American Mineralogist*, *95*(1), 185–187. https://doi.org/10.2138/am.2010.3371